Radiation Physics and Chemistry 171 (2020) 108697

Contents lists available at ScienceDirect

Radiation Physics and Chemistry

journal homepage: www.elsevier.com/locate/radphyschem

Simultaneous intramolecular crosslinking and sterilization of papain nanoparticles by gamma radiation

Gabriela N. Fazolin[a], Gustavo H.C. Varca[a,*], Lucas F. de Freitas[a], Bozena Rokita[b], Slawomir Kadlubowski[b], Ademar B. Lugão[a]

[a] Instituto de Pesquisas Energéticas e Nucleares (IPEN-CNEN/SP), Av. Prof. Lineu Prestes, nº 2242, Cidade Universitária, 05508-000, São Paulo, SP, Brazil
[b] Institute of Applied Radiation Chemistry (IARC), Lodz University of Technology, 93-950, Lodz, Wroblewskiego 15, Lodz, Poland

ARTICLE INFO

Keywords:
Nanoparticle
Papain
Gamma radiation
Protein crosslinking
Intramolecular crosslinking
Bityrosine
Disulfide bridges
Simultaneous sterilization

ABSTRACT

Papain-based nanoparticles were recently developed using radiation technologies and proven effective to generate nanosized crosslinked papain particles with preserved enzymatic activity. The applications of such nanostructured systems are expected to be similar to native papain with considerable biopharmaceutical advantages and concern drug loading among other biotechnological applications. The nature of such crosslinks and the possibility to provide simultaneous sterilization have been hypothesized but remain not totally clarified. This manuscript advances the discussion on the radiation-induced synthesis of protein nanoparticles by approaching the nature of the crosslinking and the possible contribution of bityrosine linkages and disulfide bridges to the overall nanoparticle assembly as well as the feasibility of the simultaneous sterilization process under the pre-established conditions of processing. Papain nanoparticles were synthesized and characterized according to size, proteolytic activity, bityrosine, cysteine content and molecular weight by SDS-PAGE upon sonication at 40 kHz. Bacterial identification and the sterility tests were performed in accordance with ISO 11737 prior to and after inoculating 10^6 CFU of *Corynebacterium xerosis*. Our experiments evidenced the crosslinking of rather intra- than intermolecular nature and a contribution of cysteine bridges and bityrosine linkages to the stabilization and formation of the papain nanoparticle assembly. The technique was effective to promote simultaneous crosslinking and sterilization at the established conditions of processing and may be validated in accordance with the ISO 11137.

1. Introduction

Nanocarriers have gained attention in the biomedical and pharmaceutical areas over recent years for improving drug properties and controlling drug release with reduced side effects. These nanosystems may also feature site-specific delivery, e.g., upon the attachment of particular ligands (Tarhini et al., 2017), with suitable properties for oral, nasal, intra-ocular administration, among others (Mohanraj and Chen, 2006). In general, protein-based nanoparticles are particularly special due to their biodegradability and easy alteration/modification for achieving low toxicity and suitable size for several applications, depending on the processing steps during and after synthesis. Natural proteins are obtained from animal sources, e.g., gelatin, albumin, casein, or extracted from plants, e.g., soy, zein, and papain.

Papain (EC 3.4.22.2), extracted from the latex of *Carica Papaya* Linnaeus, is a proteolytic enzyme composed of 212 amino acids divided into two domains (R, L) that hold a molecular weight of 23.4 kDa (Kamphuis et al., 1984). The enzyme features debridement and healing properties (Amri and Mamboya, 2012), anti-inflammatory, and anti-tumoral activity (Muller et al., 2016). Therefore, it holds strong potential as a drug carrier. Concerning cancer therapy, for instance, papain nanocarriers may facilitate drug permeation and increase the amount of drug delivered in the tissue, whether topically (superficial cancers) or intravenously (deep-seated tumors) administered. On the other hand, one of the most common disadvantages of protein nanoparticles refers to the risk of infection and contamination (Leo et al., 1997), which may be overcome with a sterilization step, in some cases, successfully achieved using radiation.

When it comes to polymers, radiation has been identified as a powerful tool to induce crosslinking without the need for toxic reducing agents or crosslink-inducing compounds (Ulanski et al., 1999). The same effects have been observed in proteins like bovine serum albumin (Queiroz et al., 2016) and papain (Varca et al., 2016a). The effects of the irradiation of protein especially in solution involve the generation

* Corresponding author. Centro de Química e Meio Ambiente, Brazil.
E-mail address: varca@usp.br (G.H.C. Varca).

https://doi.org/10.1016/j.radphyschem.2020.108697
Received 31 October 2018; Received in revised form 2 January 2020; Accepted 7 January 2020
Available online 08 January 2020
0969-806X/

of reactive species resultant from water or solvent radiolysis, capable of changing the protein's structure, conformation, as well as inducing detrimental effects such as degradation and overall impairment of its biological properties (Saha et al., 1995).

Besides crosslinking, radiation processing may also induce biological effects capable of sterilizing the materials depending upon processing conditions, simultaneously. Thus, radiation is often a method of choice for the sterilization of medical devices and drugs. In addition, the use of radiation technologies for the synthesis of a myriad of nanosized structures including metals and proteins, among materials has been detailed (G. G. Flores-Rojas et al., 2018).

Recent studies demonstrated that under specific conditions, radiation provides protein nanoparticle formation in a controllable size manner upon irradiation in the presence of a scavenger like ethanol or methanol (Varca et al., 2016a; Queiroz et al., 2016) and also in the absence of such compounds depending on the protein (Varca et al., 2016b). Particularly, papain nanoparticles were recently synthesized using ionizing radiation and demonstrated preserved enzymatic activity and strong potential as nanocarrier (Varca et al., 2014a; Fazolin et al., 2018).

Although such advances are relatively new, the influence of several experimental conditions for the synthesis of papain nanoparticles such as buffer molarity, temperature, ethanol concentration, as well as radiation effects regarding dose and dose rate have already been studied, and optimized parameters were already established using electron-beam (Varca et al., 2016a) and gamma irradiation (Fazolin et al., 2018). In both studies, with regard to the protein crosslinking, the linkages were hypothesized to occur via bityrosine formation, as approached by fluorescence studies.

However, the nature of such crosslinks in the stabilization or overall assembly of the papain nanoparticle, whether of intra- or intermolecular nature, as well as the role of bityrosines or disulfide bridges, remain unclarified. Also, the simultaneous sterilization effects achieved under the specific conditions of processing adopted for the synthesis of papain nanoparticles were not experimentally approached yet. On this account, this study aimed to advance the discussion regarding the nature of the crosslinking involved in the papain nanoparticle formation using the radiation-induced synthesis, identify the involvement of bityrosine and disulfide bridges, as well as provide experimental evidence of the feasibility of the simultaneous sterilization at the pre-established conditions of processing.

2. Experimental

2.1. Materials

Papain 30000 USP-U/mg (EC 3.4.22.2) and 5,5-dithiobis-2-nitrobenzoate (DTNB) were purchased from Merck (Germany). Molecular weight marker Spectra Multicolor Broad Range Protein Ladder was acquired from Thermo Scientific (USA). Ethanol, methanol, acetic acid, sodium dodecyl sulfate, monosodium phosphate, and heptahydrate disodium phosphate were acquired from Synth (Brazil). Bis-acrylamide, tris, ammonium persulfate, β-mercaptoethanol, glycerin, bromophenol blue, Coomassie blue G250, and Nα-benzoyl-DL-arginine 4-nitroanilide hydrochloride were from Sigma-Aldrich (USA). All reagents were of analytical grade.

2.2. Methods

2.2.1. Nanoparticle synthesis

Papain nanoparticles (10 mg mL^{-1}) were synthesized using 50 mM phosphate buffer in presence of 20% ethanol (v/v) on an ice bath and stored in sealed glass vials. No gas purge was performed, and samples were irradiated in atmospheric conditions. Samples were exposed to γ-radiation using ^{60}Co as a radioactive source in a Multipurpose irradiator to reach 10 kGy at a dose rate of 5 kGy h^{-1} as established by Fazolin et al. (2018).

The dosimetry was performed using Amber Perspex 3042 dyed-polymethylmethacrylate dosimeter (Harwell Dosimeters, UK). Samples were filtrated using 0.45 μm cellulose acetate syringe filters (Macherey-Nagel, Germany) and stored at 4 °C to prior analysis. Native and irradiated (10 kGy, in the absence of ethanol) papain were considered controls and were prepared and irradiated under the same conditions.

2.2.2. Nanoparticle characterization

2.2.2.1. Nanoparticle size. The hydrodynamic diameter was estimated by dynamic light scattering (DLS) on a Zetasizer Nano ZS90 device (Malvern Instruments, UK). All samples were analyzed at 20 °C using a scattering angle of 173°. The measurements were performed in 3 sets of 10 runs of 10 s each in accordance with ISO 22412. The size was reported by number.

2.2.2.2. Sonication. The samples were sonicated in the sealed glass vials at 20 °C for 2 h at a frequency of 40 kHz and 135 Watts (RMS) on an Ultra Cleaner 1400 ultrasonic bath (Unique, BR) and characterized prior to and after sonication.

2.2.2.3. Bityrosine evaluation. Fluorescence measurements were performed on a SpectraMax i3 Multi-Mode Microplate Reader (Molecular Devices, USA). Bityrosine was analyzed using excitation wavelength (λ_{Ex}) of 350 nm and emission wavelength (λ_{Em}) scanning ranging from 375 to 500 nm, excitation and emission bandwidths of 9 and 15 nm, respectively. Three scans were averaged for each spectrum.

2.2.2.4. Enzymatic activity. The proteolytic activity of papain was quantified using Nα-benzoyl-DL-arginine 4-nitroanilide hydrochloride as a synthetic substrate. Samples were properly diluted in phosphate buffer pH 7 and incubated in a thermostatic bath at 40 °C for 45 min. Absorbance was read at $\lambda = 405$ nm in SpectraMax i3 Multi-Mode (Molecular Devices, USA). The method was performed according to Ferraz et al. (2014).

2.2.2.5. Sulfhydryl content. Sulfhydryl content was determined using the Ellman's assay (Ellman, 1959). Aliquots (500 μL) of native, irradiated and nanopapain (10 mg mL^{-1}) were added to 2.5 mL of 50 mM phosphate buffer pH 8 followed by the addition of 50 μL of 0.4% DTNB, vortexing for 2 min and incubation at 20 °C for 15 min. The calibration curve was determined using cysteine solutions to obtain the standard curve of free sulfhydryl group content. The results were calculated by interpolation using the standard cysteine curve to estimate the free -SH groups. The UV absorbance measurement was performed on a SpectraMax i3 Multi-Mode Microplate Reader (Molecular Devices, USA) at 412 nm.

2.2.2.6. Molecular weight. Aliquots of papain nanoparticles (10 mg mL^{-1}) and the controls were heated up to 90 °C for 5 min and diluted in loading buffer containing β-mercaptoethanol as a reducing agent. The samples were loaded on a 12% polyacrylamide gel with a 4% stacking gel using a broad-range protein marker and assayed at 90 V and around 45 mA on a PowerPac Basic mini vertical electrophoresis device (Bio-Rad, USA) according to Laemmli (1970). The assay was also performed in non-reducing conditions, in the absence of β-mercaptoethanol.

2.2.2.7. Microbial identification. The microbial identification of the samples was performed according to the United States Pharmacopeia 40, NF 35 < 191 > (2017) using a BBL™ Crystal™ miniaturized system (BD®). After inoculation, the identification was performed in microculture in a slide and followed by optical microscopy (Lacaz et al., 1998).

2.2.2.8. Sterility testing. Nanopapain and its controls were submitted to

the sterility testing before and after inoculation with *C. xerosis* to reach a 10^6 CFU mL^{-1} from a standardized *Corynebacterium xerosis* solution (ATCC® 373™), upon irradiation. Sterility was tested by an independent accredited company (Controlbio Assessoria Técnica Microbiológica S/S Ltda., Brazil) using the direct inoculation assay as described in the Sterility Testing from the United States Pharmacopeia 31, NF 26 < 71 > (2007) and according to with ISO 11737-2:2009. The samples were inoculated on a culture medium and incubated for 14 days upon daily verification.

3. Results and discussion

3.1. Nanopapain radiation-induced synthesis and crosslinking

In the seek for a better understanding of the intra- or intermolecular nature of protein-protein crosslinks, particle size changes may provide evidence of intra- or intermolecular bonds. The size increase particularly indicates a possible intermolecular resultant from the binding of two or more molecules, while a decreased size might indicate a compact protein structure caused by the formation of bonds, indicating intramolecular linkages, or caused by molecular cleavage (Djoullah et al., 2016).

The papain nanocarrier described in this work was developed using gamma-radiation with the addition of 20% (w/w) ethanol as desolvation and scavenging agent of $OH^{\cdot}$ and other oxidizing species that are often detrimental to proteins. The role of ethanol in the process was evidenced by comparing irradiated papain in the absence and presence of ethanol. Samples irradiated in the absence of ethanol presented a marginal size increase of 0.5 nm (approximately 4 ± 1 nm), remaining with a similar size as native papain (3.4 nm ± 0.8 nm), while the samples irradiated in the presence of ethanol led to the increase in size up to 7.7 nm (± 0.9 nm) (Table 1). The irradiated controls also presented the same size as the unirradiated ones, however, bityrosine levels were considerably higher for the irradiated samples (Fig. 1), as previously reported (Varca et al., 2014b, Varca et al., 2016a).

The above-mentioned results evidenced that in the case of papain, the size changes were deeply influenced by the desolvation process caused by ethanol. The cosolvent creates a milieu proper for intra- or intermolecular recombination as pointed out in literature (Wang and Uludag, 2008), but in the case of papain, it was also crucial for the size increase. Consequently, bityrosine may not be directly linked to the size increase itself but rather to the maintenance of the structure acquired.

According to the literature, protein crosslinking by radiation occurs mainly by the linkage of two tyrosines – named di- or bityrosine (Bian and Chowdhury, 2014), derived from the damage caused by the attack of free radicals generated from the water radiolysis (Von Sonntag, 1987). The postulated mechanism for bityrosine formation was well described by Bobrowski and colleagues (Bobrowski et al., 2008), and identified to take place via one-electron oxidation, involving three main stages: abstraction of the hydrogen, recombination and the isomerization.

In the case of papain nanoparticles, the pathway for bityrosine formation is more likely to be triggered by ethanol-derived radicals, as at 20% EtOH concentration 98% of $OH^{\cdot}$ radicals are scavenged and give birth to the so-called alcohol radicals, yielded at 83%, which can abstract hydrogen atoms from protein and then trigger other reactions (Asmus et al., 1973) related to the crosslinking process (Queiroz et al., 2016; Bobrowski, 2017). The isomerization to bityrosine is favored by the absence of oxygen, which according to our calculations, begins after 1 kGy, theoretically established as the necessary dose to deplete all dissolved oxygen in the solution.

Table 1
The influence of sonication (40 kHz, 135 W) for 2 h over nanoparticle size and free sulfhydryl content for the samples irradiated at 10 kGy (^{60}Co source) in the presence of 0–20% ethanol (v/v). The particle size was determined by DLS in 3 sets of 10 runs of 12 s and the -SH content using DTNB.

Samples	Particle size (d.nm)	Free sulfhydryl content (-SH/ mol of papain)
Native Papain	3.4 ± 0.8	1.00 ± 0.10
Native Papain (sonicated)		2.00 ± 0.11
Irradiated Papain	3.9 ± 1.0	0.10 ± 0.08
Irradiated Papain (sonicated)	3.5 ± 0.9	0.10 ± 0.09
Nanopapain	7.7 ± 0.9	2.00 ± 0.11
Nanopapain (sonicated)	5.8 ± 1.2	3.20 ± 0.17

3.1.1. The role of bityrosine and disulfide bridges

3.1.1.1. Size approach. In order to experimentally support the role of disulfide bridges and bityrosines in the nanoparticle assembly, the samples were sonicated for 2 h, aiming the break of possible disulfide bridges or physical bonds, and monitored for their increase/decrease in size by DLS, towards providing evidence of the presence of inter- or intramolecular crosslinking.

Upon 2 h of sonication, the results indicated in Table 1 revealed that native papain preserved its size, while irradiated and nanopapain presented a size decrease of 0.4 nm and 1.9 nm, with an overall size of 3.5 nm and 5.8 nm, respectively, possibly suggesting that the novel linkages formed were broken. It is relevant to highlight that the increase/decrease were directly related to the ultrasound treatment time, and in the preliminary tests we did not observe a difference between samples sonicated for 15, 30, and 2 h (data not shown), and every result revealed a decrease in particle size. Such hydrodynamic diameter changes observed indicated the occurrence of intramolecular bonds involved in both nano and irradiated papain, as observed by the decrease in size after the sonication method, reinforcing the concept of intramolecular crosslinking.

The reduction in particle size refers to the cavitation and turbulent forces during the ultrasonication process, which disrupts molecular linkages (Czechowska-Biskup et al., 2005; Yanjun et al., 2014). As for papain, size changes are observed due exposures of the sulfhydryl group as the disulfide bond is broken during the sonication, reducing the SS to form SH (Hu et al., 2013; Malik et al., 2017). Also, upon sonication, proteins present a greater surface area for the source of mechanical vibrations, which makes them more susceptible to changes, such as in the particle size (Malik et al., 2017).

The ultrasound technology is, therefore, particularly useful and widely applied technique to alter protein structures and frequently used for the breakage of aggregates into smaller pieces (Stathopulos et al., 2004). This model of study was already performed for studying soy protein isolate (Arzeni et al., 2012), sunflowers protein (Malik et al., 2017), peanut protein isolate (Zhang et al., 2014) among others.

3.1.1.2. Cysteine content. Cysteine linkages may also have a role in the stabilization or maintenance of the nanoparticle structure, as additional linkages such as cysteine bonding were also postulated to take place in the crosslinking process *via* the formation of disulfide bridges (Gaber, 2005). In this case, the formation or destruction of such linkages is triggered by the aqueous electrons generated that come to contact with the protein structure and may directly affect disulfide bridges and cysteine radials (Saha et al., 1995).

The free cysteine content of each sample was quantified using the Ellman's method (Ellman, 1959). Native papain values were normalized as 1 for better comparison (Table 1). It was possible to observe that native papain presented one free sulfhydryl group, as expected, which corresponds to Cysteine 25, the only free cysteine residue present in native papain structure. The other 6 cysteine residues compose three disulfide bridges that hold the molecular assembly, along with other forces (Kamphius et al., 1984). Upon 2 h of sonication, the levels doubled, which revealed that some recombination between the cysteine residues may be taking place and that the frequency used in this

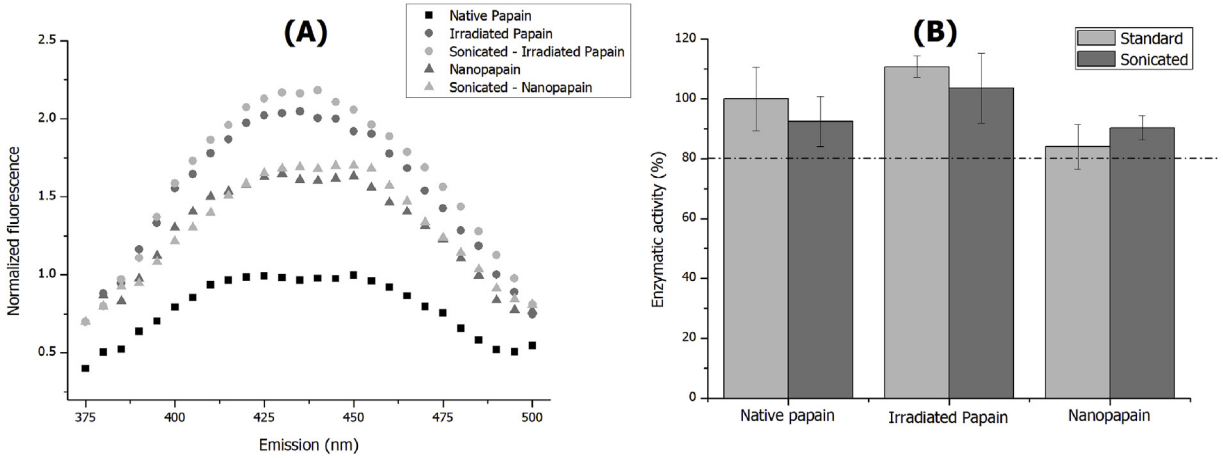

Fig. 1. Papain nanoparticles (10 mg mL^{-1}) irradiated at 10 kGy (^{60}Co source) and dose rate of 5 kGy h^{-1}. (**A**) Bityrosine emission spectra evaluated by fluorescence measurements using λ_{ex} = 350 and λ_{em} = 375–500 and (**B**) enzymatic activity of papain nanoparticles and controls measured using BAPA as a specific substrate.

sonication process is enough to lead to changes in the disulfide bridges, essential for the study.

Nanopapain featured the equivalent to two sulfhydryl groups when assayed, and upon the sonication period, the values went up, being equivalent to three free sulfhydryl groups if compared to the pristine nanopapain. This particular result suggested changes in the disulfide bridges that were followed by a loss of 1.9 nm in size upon sonication, revealing that this type of linkages may play a relevant role in the nanoparticle formation or the maintenance of the overall nanoparticle assembly, especially if no changes in the bityrosine content occur, which will be further addressed in this work.

As for the irradiated sample, no extra sulfhydryl groups were identified before and after sonication, which suggests that the structure/conformation adopted by the protein does not undergo any significant changes in the sulphydryl content upon sonication at the established conditions or it is inaccessible for a proper reaction to take place, given the new conformation acquired. Interestingly, even the signal responsible for the free cysteine, Cys-25, essential for the enzymatic activity of papain could not be traceable by the technique in the irradiated sample. Although more studies may be required for reaching a solid conclusion on the changes observed in the irradiated papain, the results were found to be suitable for the study involving nanopapain.

In comparison with BSA and whey protein, the opposite was reported. Gulseren et al. (2007) reported that the application of ultrasonication in BSA causes a change in the protein structure, increasing the surface charge and the particle size as a consequence of small aggregations, while the sulfhydryl group demonstrated significantly decrease (Gulseren et al., 2007). For concentrated whey protein, the sonication did not change the secondary structure because the SH group is located intramolecularly and makes the molecule less vulnerable to degradation upon sonication (Chandrapala et al., 2011).

3.1.1.3. Bityrosine approach. In terms of bityrosine linkages, the bityrosine emission is easily verified in protein samples by fluorescence analysis due to its emission at around 400–420 nm in a so-called non-tryptophan profile, allowing the separation of the protein signal, normally placed around λ_{Ex} 280 nm and λ_{Em} 305 nm. This emission range occurs due to the isolated ionized bityrosine chromophore, in which one of the two phenolic hydroxyl groups is dissociated (Gross and Sizer, 1959; Lehrer and Fasman, 1967).

The bityrosine crosslinking levels observed in papain nanoparticles verified by fluorescence measurements revealed that the samples sonicated for 2 h upon comparison with standard samples did not undergo any significant changes in the bityrosine profile by means of peak intensity and conformation, as observed in Fig. 1A. Such results contribute to the understanding that cysteine linkages play a role in the maintenance of the nanoparticle structure, as well as bityrosine.

However, a clear contribution of bityrosine in terms of the overall size and assembly of the nanoparticlesremained as a topic for further discussion as sonication was not capable of breaking suck linkages. Also, more information on the nature of such crosslinks is requireddespite the size experiments that evidenced an intramolecular nature, which will be clarified further in this article using the SDS-PAGE experiments.

3.1.1.4. Effects over papain proteolytic activity. Another point to consider is the enzymatic activity of papain upon sonication, especially as free sulfhydryl content changes and other mechanisms of degradation may take place. Previous studies demonstrated that the sonication process could inactivate native papain, forming aggregates, or irreversible breakdown of molecules (Feng et al., 2010). This inactivation is directly related to protein activity and might be due to the variation of secondary and tertiary structures (Yu et al., 2014).

The influence of ultrasound on the native papain structure was described (Yu et al., 2014). After the sonication treatment – under high frequency, the secondary structure was altered as a result of the damage in hydrogen bonding and van der Waals interactions (Feng et al., 2010). Some authors described that ultrasound might not be denaturing the enzymes thoroughly (Yu et al., 2014), but tryptophan residues are considerably affected by sonication. The chemical attack of ultrasound occurs via the sonolysis of water molecules that form high energy hydroxyl and hydrogen radicals generating, hydrogen peroxide (O'Donnell et al., 2010). The oxidation caused by this hydrogen peroxide might decrease fluorescence intensity (Feng et al., 2010).

Regarding the enzymatic activity of papain nanoparticles, it was observed (Fig. 1B) that the sonication method, under the conditions applied in this work, did not significantly impair the proteolytic activity of the native enzyme, the irradiated or the nanoparticulated one. Irradiated papain after sonication presented the same activity (around 100%) of the native and irradiated sample, within the standard deviation obtained in the measurements. As for sonicated nanopapain, the result showed that the enzyme still held 80% of initial activity, comparing to the native and the same activity as standard nanopapain. Some changes were observed, however, they were found to be within the standard deviation and considered null.

The free cysteine content did vary for the samples, except for the irradiated papain. However, no changes in proteolytic activity were identified as a consequence. Our understanding is that most of the changes occured rather in cysteine bonds or cysteines located outside the active site, and thus, not impairing the proteolytic activity, as expected if changes had occurred in Cysteine-25. Another aspect is that the observed variations in sulfhydryl content were associated with

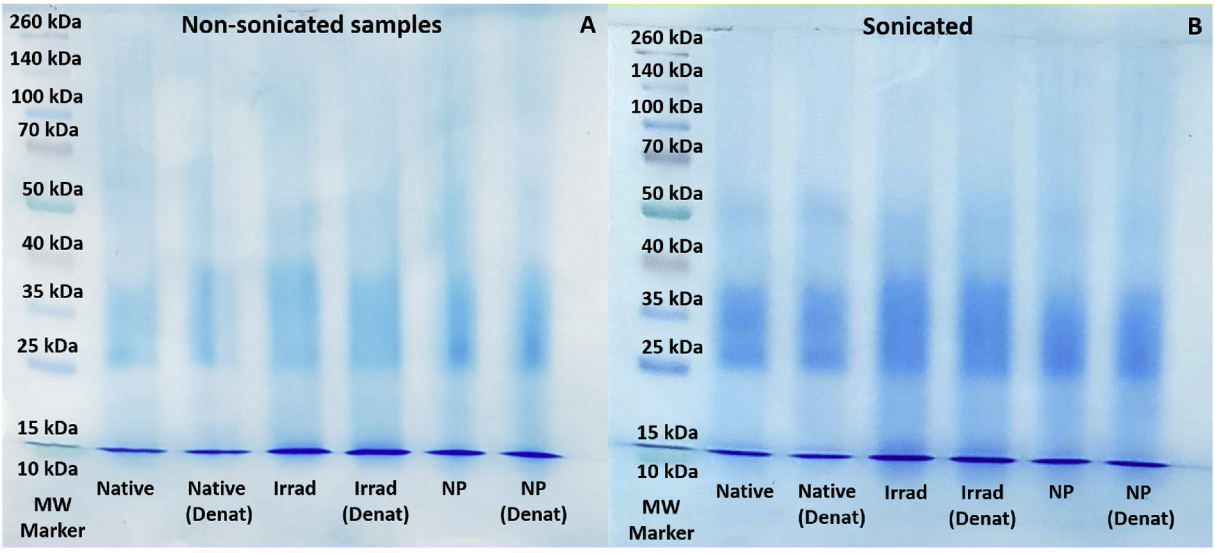

Fig. 2. 12% polyacrylamide SDS-PAGE for papain nanoparticles (10 mg mL^{-1}) irradiated on ice bath at 10 kGy and dose rate of 5 kGy h^{-1} (^{60}Co source), where MW - Molecular weight protein marker, Denat – denatured (treated with β-mercaptoethanol), and NP – nanoparticle. Sonicated samples were exposed to ultrasound for 2 h at 40 kHz and 135 W.

linkages of rather intramolecular nature, which theoretically makes them less prone to degradation upon sonication, and thus contributed to the maintenance of protein integrity and therefore, the preserved bioactivity observed.

3.1.2. *Intermolecular x intramolecular crosslinking*

3.1.2.1. SDS-PAGE. The samples were sonicated for 2 h and then assayed in the SDS-PAGE using denaturant buffer to understand and determine the nanopapain molecular weight, as the nature of the crosslinking is associated with changes in the molecular weight.

Native papain presents a molecular weight of 23.4 kDa, and as possible to visualize in Fig. 2, the bands observed for all the samples were retained near the 25 kDa region and presented a very similar profile as the native sample. No high molecular weight compounds were found after processing, as expected to occur in the case of intermolecular crosslinking.

The results mentioned above revealed and experimentally demonstrated that the nature of the crosslinking involved in the papain nanoparticle formation was not intermolecular, but rather intramolecular (understood as crosslinking inside the particle, obtained by the addition of ethanol followed by irradiation), as there is no evidence of molecular weight increase. Also, small bands were identified between 15 and 10 kDa and were attributed to papain fragments that were present as a result of a denaturation process whether induced by radiation or autolysis.

Another aspect for consideration is the increment in the retention time, which, as evidenced by Djoullah et al. (2016) may occur as a consequence of a mass increase due to the chemically-induced intermolecular crosslinking, while a decreased retention time was evidenced after the intramolecular crosslinking occurrence. The electrophoresis gel shows a slight decrease in the retention time in the nanopapain samples, especially the sonicated ones. Thus, another evidence of intramolecular crosslinking is provided.

3.2. *Simultaneous sterilization*

One of the most common claims of radiation technology when it comes to polymers, specifically hydrogels, refers to the possibility of combining simultaneous sterilization and polymer crosslinking in one single step, which depending upon the radiation source or energy, may be performed inside the final package (Rosiak, 1990). The radiation sterilization and its effectiveness are directly related to the applied dose, as well as the initial bioburden or contamination levels of a product.

When it comes to the sterilization of biomedical devices or solutions designed for direct contact with blood, a sterility assurance level (SAL) of 10^{-6} is established and the radiation process may be carried out and validated for routine processing according to ISO 11137. The standard or reference sterilization doses correspond to 15 and 25 kGy depending upon several factors, including bioburden and type of microorganism. However, validation is mandatory to assure the effectiveness of the sterilization method on a product-based approach.

3.2.1. *Microbial identification and sterility testing*

As an attempt to demonstrate and provide clear experimental evidence of the possibility to combine protein crosslinking and sterilization simultaneously under the adopted condition of processing required for the synthesis of papain nanoparticles by radiation, the microbial identification assay was performed before and after irradiation, followed by the sterility assurance test.

The presence of gram-positive bacteria of the *Corynebacterium* sp. from human skin and mucous membranes microbiota (Ellinghausen, 2011) was confirmed in the initial sample before irradiation. This is somehow expected, as they were prepared in a lab for research purposes only and not under aseptic conditions. However, as demonstrated in Table 2, after irradiation at 10 kGy under the pre-established conditions of processing, the sample was approved in the sterility test, evidencing the sterilization process taking place simultaneously to the crosslinking. Likewise, the nanopapain sample also passed the sterility assurance test, reinforcing the concept of reducing bioburden along the

Table 2
Sterility testing of the samples before and upon inoculation of 10^6 CFU mL^{-1} using *C. xerosis* culture.

Samples	Bacterial culture	Fungal culture	Result
Native papain (control)	Positive	Negative	Reproved
Native papain (with bacteria)	Positive	Negative	Reproved
Irradiated papain (control)	Negative	Negative	Approved
Irradiated papain (with bacteria)	Negative	Negative	Approved
Nanopapain (control)	Negative	Negative	Approved
Nanopapain (with bacteria)	Negative	Negative	Approved

*Test prepared in accordance with the ISO 11737-2.

process.

As the requirements for sterility reflect a SAL of 10^{-6}, we inoculated 10^6 CFU mL^{-1} of *C. xerosis* from a standardized solution using ATCC strain to the samples prior to irradiation to demonstrate and challenge the effectiveness of the method under the adopted conditions of processing, specially using highly contaminated samples. Although the initial bioburden could be considerably reduced using aseptic methods during synthesis, we selected the microorganism identified as an experimental reference to detail and assess the simultaneous sterilization.

The results revealed that after processing all samples before and upon inoculation have passed the sterility test, which provides experimental evidence of the simultaneous sterilization process. This information is particularly relevant as it confirms the hypothesis of a simultaneous crosslinking and sterilization process, postulated by previous authors (Varca et al., 2016a; Queiroz et al., 2016).

In principle, radiation sterilization is effective in terms of bioburden reduction in a range of 10^{-1} for each 2.5 kGy applied to the sample at solid state, or even more effective in the case of known contaminants or when the process is performed in liquid samples, for instance. With the radiation dose applied to 10 kGy, the samples passed the sterility test, providing clear evidence of the simultaneous sterilization even for highly contaminated samples. Nevertheless, when produced at an industrial scale, more experiments shall be performed to both minimize the initial bioburden as well as to validate the method for routine processing.

4. Conclusions

The radiation-induced synthesis of protein-based nanoparticles has been demonstrated and proven as a technique capable of inducing protein crosslinking and conferring controllable particle size at the nano level, while preserving their biological properties. In this work, we investigated the nature of the radiation-induced papain nanoparticle crosslinks, wether of intra- or intermolecular nature, as well as the possible involvement of disulfide bridges and bityrosine linkages in acquired nanoparticle assembly.

Papain nanoparticles of 7.7 ± 0.9 nm and 85% residual proteolytic activity were synthesized as described in the literature, using phosphate buffer, ethanol as a cosolvent and ^{60}Co as a radiation source to reach 10 kGy (5 kGy h^{-1}). In other words, the produced nanoparticles featured size control, preserved bioactivity, and bityrosine emission, and given the similarity with the papain nanoparticles manufactured by other authors, the samples were considered suitable for the study.

The tests performed in this work revealed that the size changes observed in the radiation crosslinked papain nanoparticles occurred as a result of the novel assembly acquired by the enzyme after desolvation and irradiation, which is maintained by linkages of rather intramolecular nature. Among the possible linkages involved in the nanoparticle formation, two were approached in this work, the disulfide bridges, and bityrosines.

The disulfide bridges were identified to play a role in over the particle size increase, as well as in the maintenance of the acquired nanoparticle assembly. As the enzymatic activity of papain, by means of proteolytic activity, was preserved after processing, such changes were more likely to occur away from the active site. On the other hand, bityrosines linkages were also present and were not affected by the ultrasonication. Such information confirmed the role of bityrosines in the maintenance of the overall nanoparticle assembly but was limited towards understanding its direct contribution to the particle size increase. Other linkages may also be present in the papain crosslinking induced by radiation, however, the techniques approached in this study were not suitable to determine the amino acids or other linkages possibly involved in the crosslinking, which remained as a topic for further investigation.

Besides the crosslinking formation, we also approached the possibility to simultaneously crosslink and sterilize the produced nanoparticles via the radiation processing, as frequently hypothesized to occur upon irradiation at a certain dose-range, but seldom experimentally demonstrated. The rationale involved a bacterial identification in the samples followed by inoculating 10^6 CFU of the respective bacterial strain (*C. xerosis)* and irradiating the sample at process conditions. After processing, the material was submitted to sterility tests using the direct inoculation assay. The results confirmed the simultaneous sterilization, even when the process was performed using highly contaminated samples. In conclusion, the radiation-induced technique effectively promoted the simultaneous intramolecular crosslinking and sterilization of papain nanoparticles, in one step, at the pre-established conditions of processing.

CRediT authorship contribution statement

Gabriela N. Fazolin: Investigation, Conceptualization, Formal analysis. **Gustavo H.C. Varca:** Conceptualization, Supervision, Writing - original draft, Writing - review & editing, Funding acquisition, Investigation, Project administration. **Lucas F. de Freitas:** Investigation, Formal analysis, Visualization, Validation. **Bozena Rokita:** Investigation, Formal analysis. **Slawomir Kadlubowski:** Conceptualization, Formal analysis, Writing - original draft, Writing - review & editing. **Ademar B. Lugão:** Conceptualization, Funding acquisition, Supervision, Project administration.

Declaration of competing interest

The authors hereby state that there are no conflicts of interest of any natured involved with or related to the work, during its conceptual, experimental and writing phase or at any other stage of its development.

Acknowledgments

The authors would like to thank Centro de Tecnologia das Radiações (CTR – IPEN-CNEN/SP) for irradiating the samples and Instituto de Química (IQ – University of São Paulo) for the DLS analysis. Dr. Pablo Vasquez and MSc. Paulo Santos for their kind contribution to the work. Regarding scholarships, we would like to acknowledge Comissão Nacional de Energia Nuclear (CNEN), and Fundação de Amparo à Pesquisa do Estado de São Paulo (FAPESP - #2015-13979-0). We also acknowledge the International Atomic Energy Agency (IAEA -CRP F22064) and Conselho Nacional de Desenvolvimento Científico e Tecnológico (CNPq - project #402887/2013-1) for the financial support provided.

References

Amri, E., Mamboya, F., 2012. Papain, a plant enzyme of biological importance. Am. J. Biochem. Biotechnol. 8, 99–104.

Arzeni, C., Martínez, K., Zema, P., Arias, A., Pérez, O.E., Pilosof, A.M.R., 2012. Comparative study of high intensity ultrasound effects on food proteins functionality. J. Food Eng. 108, 463–472.

Asmus, K.D., Moeckel, H., Henglein, A., 1973. Pulse radiolytic study of the site of hydroxyl radical attack on aliphatic alcohols in aqueous solution. J. Phys. Chem. 77 (10), 1218–1221.

Bian, S., Chowdhury, S.M., 2014. Profiling Protein-Protein interactions and protein structures using chemical cross-linking and mass spectrometry. Austin J. Biomed. Eng. 1, 1017.

Bobrowski, K., 2017. Radiation chemistry of liquid systems. In: In: Sun, Y., Chmielewski, A.G. (Eds.), Applications of Ionizing Radiation in Materials Processing Institute of Nuclear Chemistry and Technology, Warsaw.

Bobrowski, K., Houée-Levin, C., Marcianiak, B., 2008. Stabilization and reactions of sulfur radical cations: relevance to one-electron oxidation of methionine in peptides and proteins. Chimia 62, 728–734.

Chandrapala, J., Zisu, B., Palmer, M., Kentish, S., Ashokkumar, M., 2011. Effects of ultrasound on the termal and structural characteristics of protein in reconstituted whey protein concentrate. Ultrason. Sonochem. 18, 951–957.

Czechowska-Biskup, R., Rokita, B., Lotfy, S., Ulanski, P., Rosiak, J.M., 2005. Degradation of chitosan and starch by 360-kHz ultrasound. Carbohydr. Polym. 60, 175–184.

Djoullah, A., Krechiche, G., Husson, F., Saurel, R., 2016. Size measuring techniques as

tool to monitor pea proteins intramolecular crosslinking by transglutaminase treatment. Food Chem. 190, 197–200.
Ellinghausen, N., 2011. Coryneform Gram-positive rods. 10th d.J. In: In: Versalovic, K.C., Carroll, G., Funke, J.H., Jorgensen, M.L., Landry, D.W., Warnock (Eds.), Manual of Clinical Microbiology, vol. 1. ASM Press, Washington, DC, pp. 413–442.
Ellman, G.L., 1959. Tissue sulfhydryl groups. Arch. Biochem. Biophys. 82, 70–77.
Fazolin, G.N., Varca, G.H.C., Kadlubowski, S., Sowinski, S., Lugão, A.B., 2018. The effects of radiation and experimental conditions over papain nanoparticles formation: toward a new generation synthesis. Radiat. Phys. Chem. https://doi.org/10.1016/j.radphyschem.2018.08.033.
Feng, H., Barbosa-Canovas, G., Weiss, J., 2010. Ultrasound technologies for food and bioprocessing. In: In: Mawson, R., Gamage, M., Terefe, N.S., Knoerzer, K. (Eds.), Ultrasound in Enzyme Activation and Inactivation Springer, New York, pp. 369–404.
Ferraz, C.C., Varca, G.H.C., Vila, M.M.D.C., Lopes, P., 2014. Validation of in vitro analytical method to measure papain activity in pharmaceutical formulations. Int. J. Pharm. Pharm. Sci. 6, 658–661.
Flores-Rojas, G.G., López-Saucedo, F., Bucio, E., 2018. Gamma-irradiation applied in the synthesis of metallic and organic nanoparticles: a short review. Radiat. Phys. Chem. https://doi.org/10.1016/j.radphyschem.2018.08.011.
Gaber, M.H., 2005. Effect of gamma irradiation on the molecular properties of bovine serum albumin. J. Biosci. Bioeng. 100, 203–206.
Gross, A.J., Sizer, J.W., 1959. The oxidation of tyramine, tyrosine, and related compounds by peroxidase. J. Biol. Chem. 234, 1611–1614.
Gulseren, I., Guzey, D., Bruce, B.D., Weiss, J., 2007. Structural and functional changes in ultrasonicated bovine serum albumin solutions. Ultrason. Sonochem. 14, 173–183.
Hu, H., Li-Chan, E.C.Y., Zhu, L., Zhang, F., Xu, X., Fan, G., Wang, L., Huang, X., Pan, S., 2013. Effects of ultrasound on structural and physical properties of soy protein isolate (SPI) dispersions. Food Hydrocolloids 30, 647–655 I.
ISO 11137-3:2017, 2017. Sterilization of Health Care Products — Radiation — Part 3: Guidance on Dosimetric Aspects of Development, Validation and Routine Control.
ISO 11737-2:2009, 2009. Sterilization of Medical Devices — Microbiological Methods — Part 2: Tests of Sterility Performed in the Definition, Validation and Maintenance of a Sterilization Process.
ISO 22412:2017, 2017. Particle Size Analysis - Dynamic Light Scattering (DLS).
Kamphuis, I.G., Kalk, K.H., Swarte, M.B.A., Drenth, J., 1984. Structure of papain refined at 1.65 Å resolution. J. Mol. Biol. 179, 233–256.
Lacaz, C.S., Porto, E., Heins-Vaccari, E.M., Melo, N.T., 1998. Guia para identificação: fungos actinomicetos, algas de interesse médico, first ed. Editora Sarvier.
Laemmli, U.K., 1970. Cleavage of structural proteins during assembly of the head of bacteriophage T4. Nature 227, 680–685.
Lehrer, S.S., Fasman, G.D., 1967. Ultraviolet irradiation effects in poly-L-tyrosine and model compounds. Identification of bityrosine as a photoproduct. Biochem 6, 757–767.
Leo, E., Vandelli, M.A., Cameroni, R., Forni, F., 1997. Doxorubicin-loaded gelatin nanoparticles stabilized by glutaraldehyde: involvement of the drug in the cross-linking process. Int. J. Pharm. 155, 75–82.
Malik, M.A., Sharma, H.K., Saini, C.S., 2017. High intensity ultrasound treatment of protein isolate extracted from dephenolized sunflower meal: effect on physico-chemical and functional properties. Ultrason. Sonochem. 39, 511–519.
Mohanraj, V.J., Chen, Y., 2006. Nanoparticles - a review. Trop. J. Pharm. Res. 5, 561–573.
Muller, A., Barat, S., Chen, X., Bui, K.C., Bozko, P., Malek, N.P., Plentz, R.R., 2016. Comparative study of antitumor effects of bromelain and papain in human cholangiocarcinoma cell lines. Int. J. Oncol. 48, 2025–2034.
O'Donnell, C.P., Tiwari, B.K., Bourke, P., Cullen, P.J., 2010. Effect of ultrasonic processing on food enzymes of industrial importance. Trends Food Sci. Technol. 21, 358–367.
Queiroz, R.G., Varca, G.H.C., Kadlubowski, S., Ulanski, P., Lugão, A.B., 2016. Radiation-synthesized protein-based drug carriers: size-controlled BSA nanoparticles. Int. J. Biol. Macromol. 85, 82–91.
Rosiak, J., 1990. Hydrogel dressings HDR. ACS Polym. Prepr. Div. Polym. Chem. 31, 361–362.
Saha, A., Mandal, P.C., Bhattacharyya, S.N., 1995. Radiation-induced inactivation of enzymes—a review. Radiat. Phys. Chem. 46, 123–145.
Stathopulos, P.B., Scholz, G.A., Young-Mi, H., Rumfeldt, J.A.O., Lepock, J.R., Meiering, E.M., 2004. Sonication of proteins causes formation of aggregates that resemble amyloid. Protein Sci. 13, 3017–3027.
Tarhini, M., Greige-Gerges, H., Elaissari, A., 2017. Protein-based nanoparticles: from preparation to encapsulation of active molecules. Int. J. Pharm. 522, 172–197.
Ulanski, P., Rosiak, J.M., 1999. The use of radiation technique in the synthesis of polymeric nanogels. Nucl. Instrum. Methods Phys. Res. Sect. 151, 356–360.
United States Pharmacopeia, 2017. < 191 > Microbial characterization identification and strain typing. NF 40, 35.
United States Pharmacopeia, 2007. < 71 > sterelity test. NF 31, 26.
Varca, G.H.C., Ferraz, C.C.F., Lopes, P.S., Mathor, M.B., Grasselli, M., Lugão, A.B., 2014a. Radio-synthesized protein-based nanoparticles for biomedical purposes. Radiat. Phys. Chem. 94, 181–185.
Varca, G.H.C., Perossi, G.G., Grasselli, M., Lugao, A.B., 2014b. Radiation synthesized protein-based nanoparticles - a technique overview. Radiat. Phys. Chem. 105, 48–52 2014b.
Varca, G.H.C., Kadlubowski, S., Wolszczak, M., Lugão, A.B., Rosiak, J.M., Ulanski, P., 2016a. Synthesis of papain nanoparticles by electron beam irradiation – a pathway for controlled enzyme crosslinking. Int. J. Biol. Macromol. 92, 654–659.
Varca, G.H.C., Queiroz, R.G., Lugão, A.B., 2016b. Irradiation as an alternative route for protein crosslinking: cosolvent free BSA nanoparticles. Radiat. Phys. Chem. 124, 111–115.
Von Sonntag, C., 1987. The Chemical Basis of Radiation Biology. Taylor & Francis, London, NY.
Wang, G., Uludag, H., 2008. Recent developments in nanoparticle-based drug delivery and targeting systems with emphasis on protein-based nanoparticles, Expert Opin. Drug Deliv. 5, 499–515.
Yanjun, S., Jianhang, C., Shuwen, Z., Hongjuan, L., Jing, L., Lu, L., Uluko, H., Yanling, S., Wenming, C., Wupeng, G., Jiaping, L., 2014. Effect of power ultrasound pretreatment on the physical and functional properties of reconstituted milk protein concentrate. J. Food Eng. 124, 11–18.
Yu, Z.-L., Zeng, W.-C., Zhang, W.-H., Liao, X.-P., Shi, B., 2014. Effect of ultrasound on the activity and conformation of α-amylase, papain and pepsin. Ultrason. Sonochem. 21, 930–936.
Zhang, Q.T., Tu, Z.C., Xiao, H., Wang, H., Huang, X.Q., Liu, G.X., Liu, C.M., Shi, Y., Fan, L.L., Lin, D.R., 2014. Influence of ultrasonic treatment on the structure and emulsifying properties of peanut protein isolate. Food Bioprod. Process. 92, 30–37.